

Supplementary Materials: AAV-CRISPR/Cas9 Gene Editing Preserves Long-Term Vision in the P23H Rat Model of Autosomal Dominant Retinitis Pigmentosa

Saba Shahin, Hui Xu, Bin Lu, Augustus Mercado, Melissa K Jones, Benjamin Bakondi and Shaomei Wang

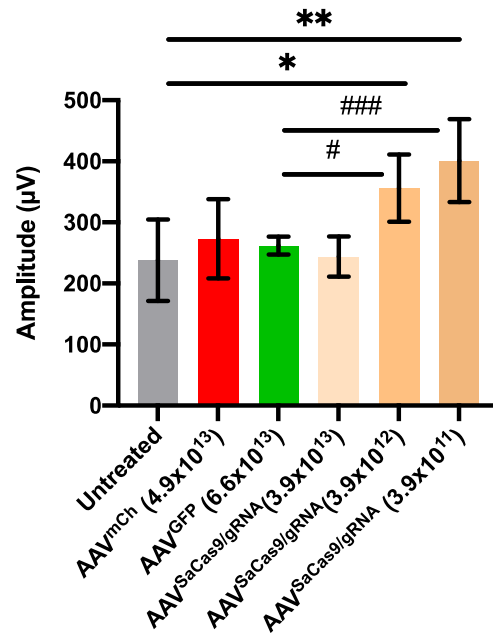


Figure S1. AAV controls. To assess AAV toxicity and determine optimal dose, P15 P23H/SD rats received a single unilateral trans-scleral subretinal injection of 2µl AAV at concentrations of 3.9×10^{13} GC/ml ($244 \pm 33\mu V$, $n = 14$), 3.9×10^{12} ($356 \pm 55\mu V$, $n = 3$), or 3.9×10^{11} ($401 \pm 68\mu V$, $n = 3$) (orange bars), and control rats received either AAV8.CMV-mCherry (AAVmCh 4.9×10^{13} GC/ml, red bar), or AAV8.CMV-GFP (AAVGFP 6.6×10^{13} GC/ml, green bar), or left untreated (untreated controls: grey bar). ERG at P90 showed that retinal perturbation from AAV controls significantly reduced visual function, whereas AAV containing SaCas9/gRNA showed improved visual function and had no deleterious effect compared to sham-operated eyes. Dosages are shown as genome copies (GC) per microliter. Data represents the mean \pm SEM. $^{\#}p \leq 0.05$, $^{\#\#\#}p \leq 0.01$; $^*p \leq 0.05$, $^{**}p \leq 0.001$.

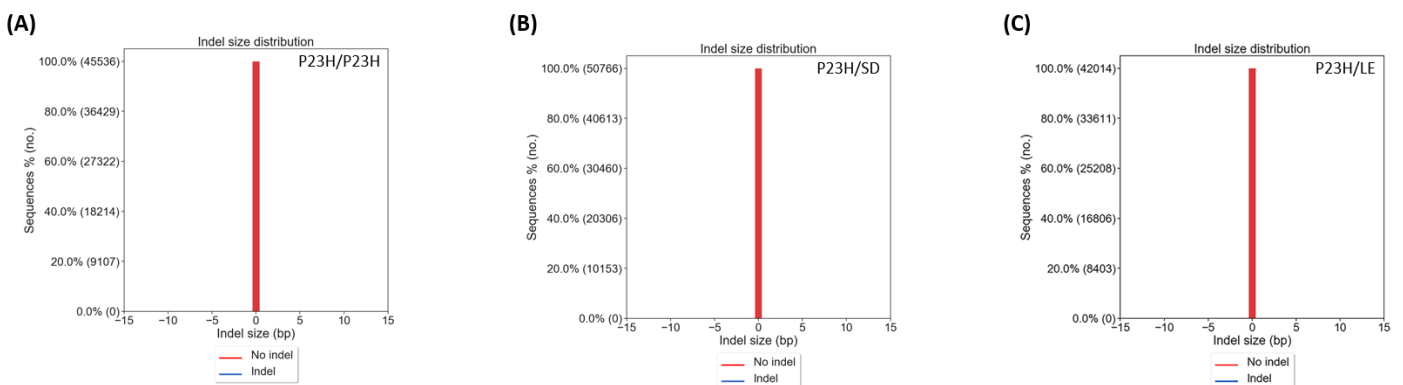


Figure S2. Indel profile of untreated controls: Representative graphs showing the frequencies and distributions of indels in untreated P23H [P23H/P23H (A), P23H/SD (B) and P23H/LE (C)] rats. No insertion and/or deletion were detected at predicted cleavage site of the targeted region.

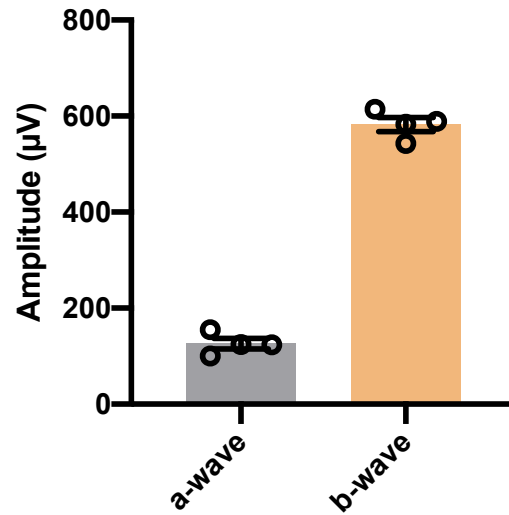


Figure S3. Electroretinography (ERG) of wild type Long Evans (LE) rats: Four adult LE rats, both male and female were dark-adapted overnight. ERG response amplitudes to full field light stimulation were recorded. ERG showed no change in a-wave ($125.96 \pm 11.26 \mu\text{V}$) and b-wave ($582.26 \pm 14.69 \mu\text{V}$) in these four LE rats of different ages (P124, P154 and P284). Data represents the mean \pm SEM ($n = 4$).

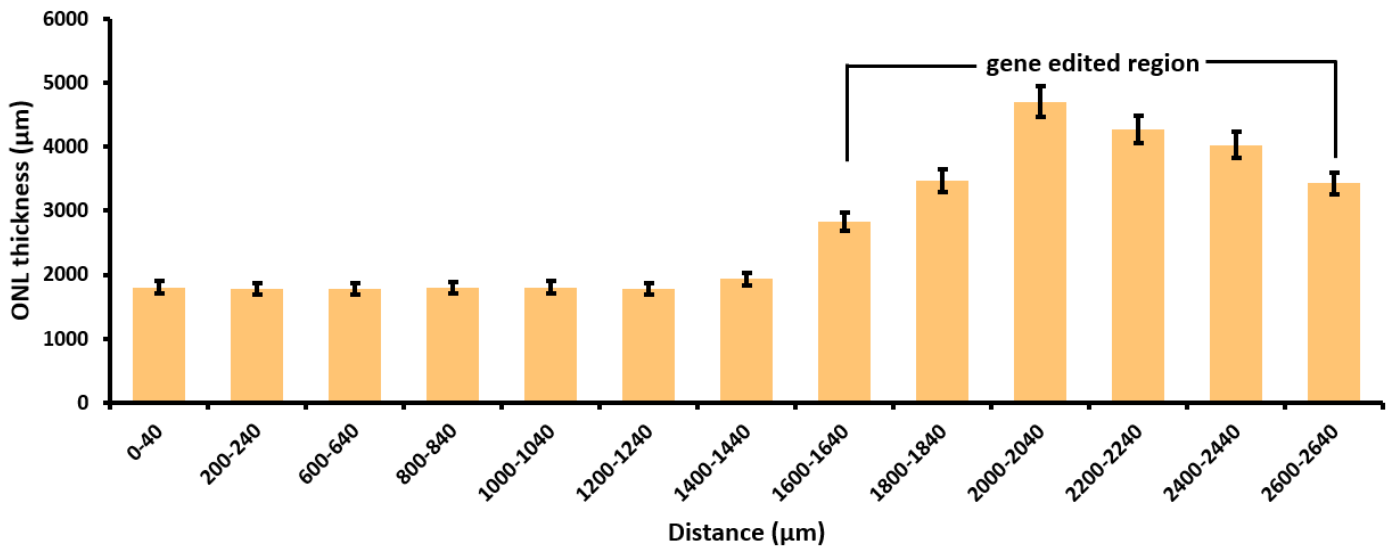
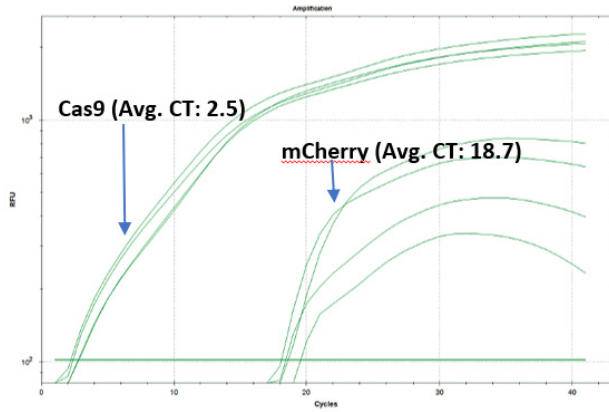


Figure S4. Quantification of ONL thickness along its rostral-caudal axis up to 2640 μm in the AAV-treated retina: ONL rescue was documented in the gene edited region (from 1600 μm to 2640 μm) that clearly demonstrates photoreceptor rescue in this gene edited region of the AAV-treated retina.



	Ct values	avg.Ct	deltaCt	RQ
CMV-mCherry1	19.58	18.695	16.1525	72,843
CMV-mCherry2	18.09			
CMV-mCherry3	18.39			
CMV-mCherry4	18.72			
ntc	0			
mOp500-SaCas1	2.85	2.5425		
mOp500-SaCas2	2.79			
mOp500-SaCas3	2.34			
mOp500-SaCas4	2.19			
ntc	0			

Figure S5. Assessment of AAV packaging efficiency. Real-time PCR amplification showing AAV packaging frequency of mCherry compared with SaCas9 transcripts. Cycle Threshold (CT) values are shown for amplified vector regions spanning the mOp500 promoter and SaCas9 (avg. CT: 2.5), or CMV promoter and mCherry transcripts (avg. CT: 18.7). Relative quantification (Δ CT: 16.15) indicated that the SaCas9 transcript was 7.2×10^4 -fold more abundant than mCherry. RT-PCR was performed in quadruplicate using SYBR-green detection. Primer sequences are as follows: CMV-mCherry: Forward primer GTAACAACCTCCGCCCATTT, Reverse primer: ATGGCCATGTTATCCTCCTC; mOp500-SaCas9: Forward primer GGGTCAGTGCCTGGAGTT, Reverse primer: ATACCGACCTTCCGCTTCT.

Table S1. Predicted on- and off-targets sites for gRNA.

	Target Sequence	PAM	Mis-match	Fwd Priming Site	Rev Priming Site
OFF-T1	TGGaCCCAAGAaacAG-cAGCCA	GGGAG T	5	GGAAAACACAGTGC-TACAGTC	TCAGGAA-GAGGTTTCATGGT
OFF-T2	TaGGCCCAAAtAttAtGTAGCCA	GTGAG T	5	TTCTCTCAACGGG-GATTGAC	GACATTAGGAGCCAC-CTACC
OFF-T3	TGtGCaCAAAtACacAG-TAGCCA	AA-GAGT	5	GAGCTG-TACACAGGTCTAGC	GAAGGACAGCAGA-GAGCTAA
ON-T	TGGGCCCAAAGAC-GAAGTAGCCA	TGGAG T	0	ACAGAGGGCCCCAATTT TTA	CCCAG-TCTCTCTGCTCATAC

Table S2. Primer sequences used for qPCR.

Gene	Sense (5'-3')	Antisense (5'-3')	Accession Number
<i>r-Atf6</i>	ATGGAGTCGCCTTTTAGTCC	CTGTACCGACTCAGGGAGGG	NM_001107196.1
<i>r-Atg5</i>	ACCTCGGTTTGGCTTGGTTG	AGTATGGCTCTGCTTCTCGTT	NM_001014250.1
<i>r-Atg7</i>	AGCCTGTTTCATCCAAAGTTCT	CTGTGGTTGCTCAGACGGT	NM_001012097.1
<i>r-Becn1</i>	GCGTCGGGGCCTAAAGAATG	CTCCTGGCTCTCCTGGTT	NM_053739.2
<i>r-BiP</i>	GACCACCTATTCTGCGTCGGT	CGCCAATCAGACGCTCCCCT	NM_013083.2
<i>r-Chop</i>	AGGAGAGAGAAACCGGTCCAA	GGACACTGTCTCAAAGGCGA	NM_024134.2
<i>r-Gapdh</i>	ACAGCAACTCCCATTCTTCCA	TCCAGGGTTTCTTACTCCTTGG	NM_017008.4
<i>r-Gnat1</i>	TGACGTGCATCATTTTCATC	TTAAGCTCCAGGAAGTGCAC	NM_001108780.2
<i>r-Perk</i>	GAAGTGGCAAGAGGAGATGG	GAGTGGCCAGTCTGTGCTTT	NM_031599.2
<i>r-Rho</i>	GTCCACTTCACCATCCCC	CTGCCTTCTGAGTGGTAGCC	NM_033441.1
<i>m-Rho</i>	ACAGTCAAGGAGGCGGCT	GCAAAGAAAGCTGGCAGAG	NM_145383.2

Table S3. Frequency of indels and frameshift in AAV-SaCas9/gRNA treated and untreated P23H rats.

Genotype	Groups	Number of Total Target Reads	Number of Reads with Indels	Frequency of Indels (%)	Number of Frameshift Reads	Frequency of Frameshift (%)
P23H/P23H	Untreated	44782	0	0.00	5	0.01
	AAV-treated	131250	6404	4.88	7596	5.78
P23H/SD	Untreated	50766	0	0.00	1	0.06
	AAV-treated	119481	13019	10.89	15032	12.58
P23H/LE	Untreated	42014	0	0.0	1	0.00
	AAV-treated	167609	21705	12.95	24375	14.54

Table S4. Off-target analysis of CRISPR/Cas9-mediated editing of *m-Rho^{P23H}* in P23H rats.

Genotype	Groups	Off-Target 1		Frequency of Indels (%)	Off-Target 2		Frequency of Indels (%)	Off-Target 3		Frequency of Indels (%)
		Number of reads with indels	Number of total target reads		Number of reads with indels	Number of total target reads		Number of reads with indels	Number of total target reads	
P23H/P23H	Untreated	0	149598	0	0	128268	0	0	141561	0
	AAV-treated	0	117695	0	0	102693	0	0	151268	0
P23H/SD	Untreated	0	103016	0	0	143373	0	0	153068	0
	AAV-treated	0	76721	0	0	136605	0	0	65796	0
P23H/LE	Untreated	0	55228	0	0	105284	0	0	201194	0
	AAV-treated	0	26572	0	0	133679	0	0	156138	0